IJMMM
International Journal of
Minerals, Metallurgy and Materials
矿物冶金与材料学报（英文版）

Rheological behavior of paste in metal mines

Aixiang Wu, Zhuen Ruan, and Jiandong Wang

Cite this article as:
Aixiang Wu, Zhuen Ruan, and Jiandong Wang, Rheological behavior of paste in metal mines, *Int. J. Miner. Metall. Mater.*, 29(2022), No. 4, pp. 717-726. https://doi.org/10.1007/s12613-022-2423-6

International Journal of Minerals, Metallurgy and Materials
Volume 29, Number 4, April 2022, Page 717
https://doi.org/10.1007/s12613-022-2423-6

Invited Review

Rheological behavior of paste in metal mines

Aixiang Wu[1)], *Zhuen Ruan*[1,2,3),✉], *and Jiandong Wang*[1,3)]

1) Key Laboratory of High-Efficient Mining and Safety of Metal Mines of the Ministry of Education, University of Science and Technology Beijing, Beijing 100083, China
2) Shunde Graduate School of University of Science and Technology Beijing, Foshan 528399, China
3) School of Civil and Resources Engineering, University of Science and Technology Beijing, Beijing 100083, China

(Received: 13 December 2021; revised: 15 January 2022; accepted: 18 January 2022)

Abstract: Cemented paste backfill (CPB) has been one of the best practical approaches for tailings management and underground goaf treatment. Paste rheology is a science to study the flow and deformation behaviors of paste or filling body under the effects of stress, strain, temperature, and time during the CPB process. The goal of studying paste rheology is to solve the engineering problems existing in four key processes; that is, paste rheology should meet the engineering demands of thickening, mixing, transportation, and backfilling. However, paste rheology is extremely complicated due to its high concentration, materials complexity, and engineering characteristics of non-stratification, non-segregation, and non-bleeding. The rheological behavior of full tailings in deep thickening, rheological behavior of paste in mixing and pipeline transportation, and rheological behavior of filling body are introduced and discussed: (1) gel point, compressive yield stress, and the hindered settling function are adopted to characterize the rheological properties of full tailings in deep thickening. Combination of Coe–Clevenger theory and Buscall–White theory can also analyze the thickening performance in the whole area of deep cone thickener; (2) yield stress and viscosity are consistent with the evolution trend of the relative structure coefficient of paste in mixing; (3) coupling effect of wall slip and time–temperature dependency has a significant influence on the rheological properties and pipeline transportation; (4) damage variable is introduced to the Burgers model to describe the creep damage of the filling body. However, in-depth and systematic studies were still needed to establish a complete theoretical system of paste rheology in metal mines.

Keywords: paste rheology; cemented paste backfill; thickening; mixing; pipeline transportation

1. Introduction

As important natural resources that human beings depend on for survival, mineral resources are the basis of human social and economic development. However, the mining industry has resulted in serious safety and environmental issues [1–4]. With the development of global mining science and technology, especially the innovation of tailings thickening and high concentration slurry pipeline transportation, cemented paste backfill (CPB) has been one of the best practical approaches for tailings management and underground goaf treatment [5–8]. Moreover, CPB has become an essential method for green mining in China because of its advantages of being safe, environmental, economical, and highly efficient [6,7,9–10]. CPB can use solid waste in mines (tailings) to treat the two major hazardous sources (underground goaf and surface tailings pond caused by mining), achieving the goal of "one waste to cure two harms" [6,11].

Paste, a type of toothpaste-like structure fluid with non-bleeding, is made of multiscale granular materials and water, as shown in Fig. 1. According to available data, more than 200 metal mines are estimated to have adopted or are building CPB systems [6–7]. The typical flow-process diagram of CPB in metal mines is illustrated in Fig. 2 [6–7,11–13].

CPB in metal mines mainly consists of four key processes: full tailings thickening, multiscale aggregate mixing, paste pipeline transportation, and paste backfilling and consolidation in underground goaf. The low-concentration tailings slurry discharged from the minerals processing plant is first thickened and then mixed with cementing materials (e.g., cement), coarse aggregates (e.g., waste residue, gravel), and other materials to prepare paste slurry. After mixing preparation, the paste is then transported to the underground goaf for backfilling through pipelines by gravity or pumping. In underground goaf, paste slurry solidifies and hardens into filling body. According to the National Standard of the People's Republic of China (GB/T 39489—2020), the technical indexes of CPB should meet the requirements shown in Table 1 [13].

Although CPB has been widely used in China, its theoretical foundation is still relatively weak, limiting the development of essential technology and equipment. In thickening, the tailings slurry concentration increases from less than 30wt% to approximately 70wt% after flow through the deep cone thickener (DCT, also called paste thickener), and the tailings slurry changes from solid–liquid two-phase flow to non-Newtonian fluid after flocculation, settling, sedimenta-

✉ Corresponding author: Zhuen Ruan E-mail: ustb_ruanzhuen@hotmail.com

Fig. 1. Paste with characteristics of non-stratification, non-segregation, and non-bleeding.

tion, and shearing [14–20]. In mixing, solid particles (cement, coarse aggregates, chemical additives, and other materials) must be uniformly dispersed in non-Newtonian thickened tailings slurry under the effects of convective motion, diffusion, and shearing; the materials also transform from loose solid or thickened slurry into a homogeneous paste with good fluidity [21–23]. In pipeline transportation, the prepared paste slurry should be transported to the underground goaf stably and continuously; pipeline vibration, pipeline plugging, pipeline wearing, and pipeline explosion should be reduced or even avoided by controlling the flow behavior of paste [9,24–27]. To effectively control ground pressure and strengthen mining in the backfilling and solidification links, ensuring a uniform distribution of filling body strength and adequate roof contact and control deformation creep in the filling body is necessary [28–31].

Therefore, the flow and deformation behaviors of the paste or filling body should be investigated to understand the mechanism of the CPB process. At the same time, rheology is the study of the deformation and flow of matter [32]. Accordingly, it is rheology that provides a theoretical foundation for the four key processes in CPB.

This paper gives a systematic introduction of paste rheology in metal mines. The rest of the paper is structured as follows: Section 2 introduces the framework of paste rheology in metal mines. Section 3 discusses the complexity of paste rheology. Sections 4, 5, 6, and 7 present and discuss the rheological behavior of full tailings in deep thickening, paste in mixing, paste in pipeline transportation, and the filling body, respectively. Section 8 concludes the study and describes future work in paste rheology in metal mines.

2. Framework of paste rheology in metal mines

Paste rheology is a science to study the flow and deformation behaviors of paste or filling body under the effects of

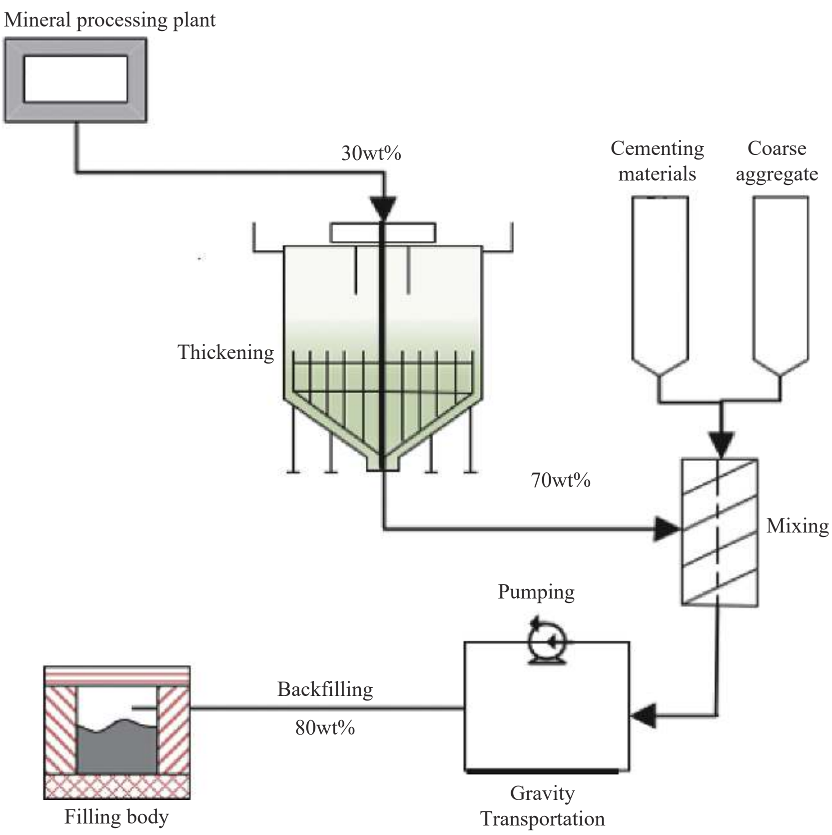

Fig. 2. Typical flow-process diagram of CPB in metal mines.

Table 1. Technical indexes of CPB

Bleeding rate / %	Slump / mm	Yield stress / Pa	Setting time / h	Uniaxial compressive strength / MPa
1.5–5	180–260	100–200	>8	0.2–5

stress, strain, temperature, and time during the CPB process. It is a branch of rheology with the particularity and complexity of the mining industry. The framework of paste rheology in metal mines is shown in Fig. 3 [12]. Based on rheology theory, the main research content of paste rheology is the constitutive equation of paste. The research methods comprise theoretical study, rheological experiments, and numerical calculation. Moreover, artificial intelligence (AI) modeling has increasingly become an important research approach in CPB [33–34]. The goal of studying paste rheology is to solve the engineering problems existing in four key processes; that is, paste rheology should meet the engineering demands of thickening, mixing, transportation, and backfilling.

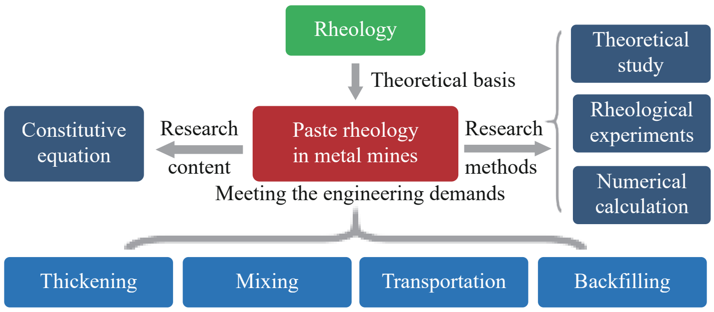

Fig. 3. Framework of paste rheology in metal mines.

3. Complexity of paste rheology

3.1. High concentration

The paste concentration can generally reach approximately 80wt%, which is much higher than that of low-concentration tailings slurry [15,27,35]. Determining whether the solid particles are dispersed in the water or the water is dispersed in the solid particles at such a high concentration is difficult. In comparison, the traditional solid–liquid two-phase flow is a dispersion system with water as the dispersion medium and solid particles as the dispersion substance. Paste has high viscosity and plasticity (yield stress) without an obvious critical flow rate and critical concentration during pipeline transportation. Its pipeline transportation shape is non-Newtonian fluid, with obvious plug flow (also called plunger flow) characteristics [6,9,36]. Under the high concentration condition, the paste slurry produces a non-negligible 3D (3-dimension) structure among particles. Calculating the interaction between particles and fluids using the formulas of resistance and lift force under the two-phase flow model is difficult [37].

For example, the two-phase flow theory cannot explain the friction effect between particles and the rheological behavior of non-Newtonian suspension substrate formed by fine particles (tailings and cement particles). Therefore, high concentration is an important reason for the complex rheological behavior of paste slurry.

Moreover, high concentration makes it difficult to determine the paste flow model. High concentration slurry has strong non-Newtonian fluid flow characteristics during pipeline transportation. The flow model of paste is different from the traditional model of solid–liquid two-phase flow. The corresponding shear-induced migration of particles must be considered in determining the flow model of the paste slurry during pipeline transportation. Consideration must be given to whether the plug flow model can continue to be adopted or not, whether the coarse particles have radial movement during transportation, and related movement rules are required or not [38–39]. All these factors must be considered when determining the paste slurry flow model due to high concentration [38–41].

3.2. Complexity of paste slurry materials

The complexity of paste slurry materials is mainly reflected in the physical and chemical properties of slurry materials [11–12,32,37].

(1) Complexity of physical properties.

The composition, size, and shape of particles in paste are more complicated than traditional suspensions, leading to the complexity of paste rheology [37,42]. Paste slurry comprises tailings particles, cementing materials, coarse aggregates, water, and chemical additives. Moreover, the composition of tailings in each mine is not the same. At the same time, the particles in paste have the characteristics of multiple scales, from a few microns to a few hundred microns. The upper limit of particle diameter can also reach a centimeter level when coarse aggregates are added. The tailings particles are irregular (not spherical or ellipsoidal), and the shape of solid particles is different.

(2) Complexity of chemical properties.

The chemical composition, hydration reaction, and chemical action of additives in paste slurry are also more complicated than traditional rheological objects, aggravating the complexity of paste rheology [37]. The chemical composition of the tailings from each mine is different. In the case of small particle size, the difference in chemical composition greatly impacts the rheological property of paste slurry. Moreover, flocculant, cement, superplasticizer, and other chemical additives are added during the CPB process, causing chemical reactions and changes in the 3D structure of the slurry.

The complexity of paste slurry materials leads to difficulty in the rheological measurement of paste slurry [37,43–45]. The complexity of paste slurry material composition makes it difficult to guarantee the repeatability of paste slurry rheological test samples and the uniformity of the distribution of components inside the sample during measurement, especially in the rheometer when measuring the yield stress of the slurry. The problem of repeatability affected by slurry composition and the problem of uniformity affected by the mixing effect during sample preparation can lead to some differences in the internal 3D structure. Such differences directly affect the measurement results of the yield stress of the CPB slurry.

3.3. “Three non” engineering characteristics

Compared with the traditional low-concentration tailings slurry, paste has “three non” engineering characteristics: non-stratification, non-segregation, and non-bleeding [11–12, 37,46]. Based on the “three non” engineering characteristics of paste, the paste slurry is obviously no longer an ordinary solid–liquid two-phase flow. For no-stratification characteristics, the paste slurry is a non-Newtonian fluid with yield stress. Under static conditions in the underground goaf, the coarse particles do not have settlement movement in the vertical direction, and critical yield stress exists. For non-segregation characteristics, the coarse particles moving synchronically with the non-Newtonian suspension substrate comprises fine particles of tailings, and the segregation led by the separation of the coarse particles from the non-Newtonian suspension substrate does not occur. For non-bleeding, the paste slurry has a 3D structure inside, the pore connectivity between the 3D structures is dense, and the internal water in the 3D structure does not flow easily.

To realize the “three non” engineering characteristics of paste slurry, studying the 3D microstructure of complex fluids and the movement of particles in complex fluids is necessary. The rheology of paste in metal mines has obvious industry particularity compared with traditional rheology. However, investigating the microscopic 3D structure and the coarse particles of the paste slurry is difficult. Therefore, the rheological behavior of paste in CPB is complex. Moreover, exploring paste rheology in metal mines is difficult due to high concentration, complexity material composition, and the “three non” engineering characteristics.

4. Rheological behavior of full tailings in deep thickening

The deep thickening of full tailings in DCT is illustrated in Fig. 4. In deep thickening, the form of tailings changes from solid particle to floc and even the floc network, with the concentration in DCT increasing from 30wt% to approximately 70wt%.

4.1. Rheological properties of full tailings in deep thickening

Gel point, compressive yield stress, and the hindered settling function are adopted to characterize the rheological properties of full tailings in deep thickening [47–49]. Gel point and compressive yield stress can characterize the degree of the dewatering of the flocs. The hindered settling function can characterize the dewatering speed of the flocs.

Fig. 4. Schematic of the deep thickening of full tailings in DCT.

Gel point is the critical concentration that flocs begin to touch each other and is the concentration at the beginning of the compression zone [50]. The compressive yield stress refers to the stress that must be applied to increase the slurry concentration further when the slurry network structure yields and compresses at a certain concentration [47,49]. The hindered settling function is determined, as shown in Eq. (1) [47].

$$R(\phi) = \left(\lambda / V_{\mathrm{p}}\right) \frac{u_{\mathrm{st}}(1-\phi)}{u} \tag{1}$$

where $R(\phi)$ is the hindered settling function, Pa·s·m^{-1}; ϕ is the solid volume fraction, %; λ is the Stokes drag coefficient; V_{p} is the volume of the particle (floc), m^3; u is the settling velocity under different concentrations, m·s^{-1}; u_{st} is the Stokes settling velocity, m·s^{-1}.

Gel point varies with the rotational speed of the rake [12,51]. According to the small-scale dynamic thickening experiment results using the full tailings from a copper mine, gel point significantly increases during the sedimentation process under the effect of shear. Gel point first increases and then decreases as the rake speed increases, reaching a maximum of 61.8wt% at the rake speed of 0.13 rad/s [12,51]. The floc network structure is broken under shear, and the internal water is discharged. The floc size then becomes small, and the floc network structure is compacted, resulting in an increase in concentration. However, when the rotational speed of the rake is higher than 0.13 rad/s, the flocs are mixed with water, and the gel point decreases slightly [12,51].

At the same time, the compressive yield stress and hindered settling function are considered functions of the solid volume fraction in underflow [12,51–53]. The functions are shown as Eqs. (2) and (3), respectively [12,51].

$$p_{\mathrm{y}}(\phi) = \left(\frac{a\left(\phi_{\mathrm{cp}}-\phi\right)\left(b+\phi-\phi_{\mathrm{g}}\right)}{\left(\phi-\phi_{\mathrm{g}}\right)}\right)^{-k} \tag{2}$$

$$R(\phi) = r_a(\phi - r_g)^{r_n} + r_b \quad (3)$$

where a, b, k, r_a, r_b, r_g, and r_n are the fitting parameters; ϕ_{cp} is the limiting volume fraction of tailings; ϕ_g is gel point.

4.2. Relationship between the rheological properties and microstructure of thickened tailings

As displayed in Fig. 5, the compressive yield stress increases with the underflow concentration, whereas the pores in thickened tailings become less when the underflow concentration rises. When the underflow concentration is 55.8wt%, the pore structure is mainly parallel plate pores with openings on all sides. It is the main part of the water channel and has good connectivity with the surrounding pores. The strength of the network is low, which shows low compressive yield stress (10.25 kPa). The pore structure is mainly tree-branch-shaped pores with both ends open when the underflow concentration rises to 58.7wt%. This kind of pore is located at the network node. It has a high degree of connectivity with the upper and lower pores. It also has many connected positions and is an important part of the water channel. The strength of the network is low, which suggests low compressive yield stress (10.57 kPa). When the underflow concentration is 63.4wt%, the pore structure comprises cylindrical pores with one end closed and wedge-shaped pores or conical pores with one end closed. The pores are located at the network's edge, forming a local water channel. Under a stable state, the water in the slurry is difficult to drain, and the network strength is large, which indicates that the compressive yield stress is large (11.09 kPa). When the underflow concentration reaches 66.2wt%, the pores are relatively independent, and forming a drainage channel is difficult. The liquid in the dense slurry is isolated by solid particles, and the strength of the particle network is high, which represents high compressive yield stress (11.45 kPa). We can conclude that the more obvious the pore microstructure is, the smaller the compressive yield stress of thickened tailings is, whereas the worse the pore microstructure is, the larger the compressive yield stress is.

4.3. Deep thickening mechanism of full tailings based on rheological properties

In the settling area of DCT, the settling rate of solid is only a function of the concentration. It has no mechanical relationship with the floc groups in the lower part (compression area) of DCT. The solid settling rate can be obtained from Coe–Clevenger theory (C–C theory) [54], in which the interactions among flocs are ignored. The solid flows through the compression area when the concentration is larger than the critical concentration. In the compression area, flocs form a continuous network structure, resulting in the particle migration being affected by gravity and structural force. The settling rate of particles is no longer related to the concentration only. The settling and thickening process in this area can be described by Buscall–White theory (B–W theory) [48], in which the compressive yield stress and the hindered settling function are considered.

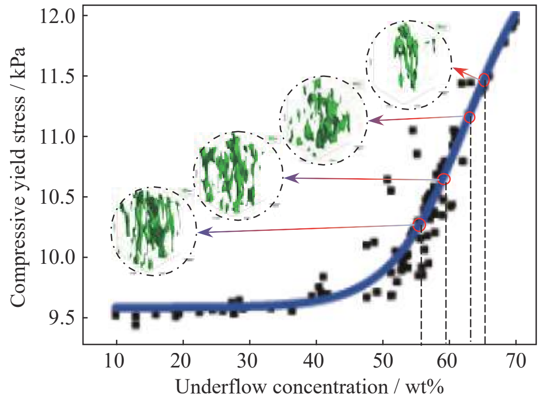

Fig. 5. Relationship between the rheological properties and microstructure of thickened tailings (green represents pores in thickened tailings) (modified from [12]).

To describe the deep thickening of full tailings in DCT, we can take the gel point as the separatrix and use C–C theory to analyze the area when the concentration is smaller than the gel point, and then apply B–W theory to explore the area when the concentration is larger than the gel point. By combining these two theories, we can analyze the thickening performance in the whole area of DCT, as displayed in Fig. 6 [47].

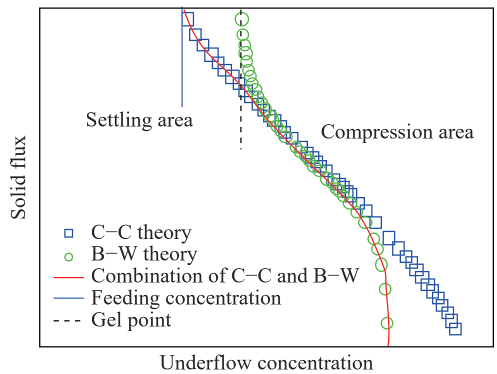

Fig. 6. Combination of C–C theory and B–W theory.

5. Rheological behavior of paste in mixing

In paste mixing, ultrafine cement particles are not easy to disperse in high concentration and high-viscous thickened tailings, as illustrated in Fig. 7. To obtain homogenization fluidization paste, a horizontal double-shaft mixer is widely used. Solid and slurry move circularly in the horizontal double-shaft mixer; subsequently, a homogeneous paste slurry is obtained, as shown in Fig. 8.

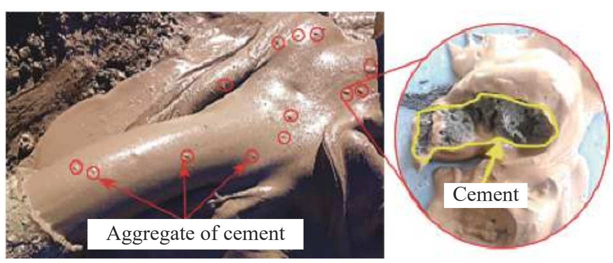

Fig. 7. Aggregate of cement in paste.

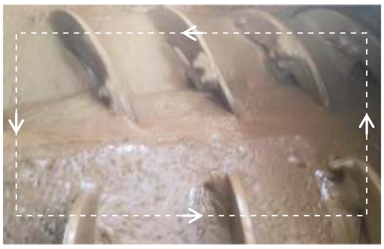

Fig. 8. Paste mixing in a horizontal double-shaft mixer.

5.1. Influence of mixing on the microstructure of paste

The microstructure of paste during mixing obtained by a particle video microscope is shown in Fig. 9 [12]. Paste is a network consisting of aggregates of various sizes and some particles during mixing. Many aggregates are formed by tailings and cement particles. At the same time, there still exist some pores (blue) among the aggregates. Moreover, the aggregates become small with continuous mixing, indicating that the ultrafine cement particles disperse in the thickened tailings evenly. In general, the effect of shearing on the microstructure of the paste is characterized by the evolution of the pore structure. Fig. 9(a) displays that when cement is added and mixed for 10 s, large red blocks (cement) and a few pores (water) exist, resulting in high structural strength. Fig. 9(b) and (c) illustrate that the cement gradually disperses and the pore distribution is uniform as the mixing time increases, suggesting that the strength of the structure decreases.

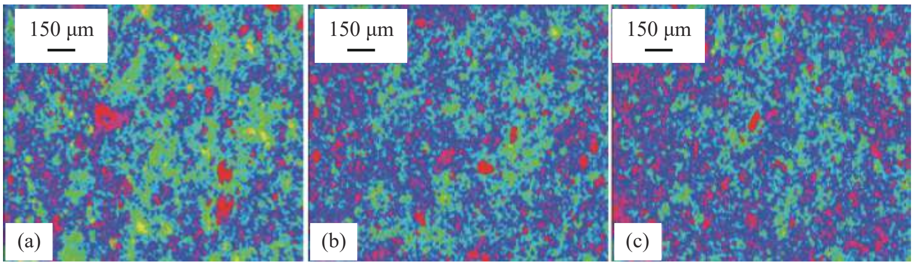

Fig. 9. Microstructure of paste during mixing: (a) 10 s; (b) 180 s; (c) 300 s. Red, blue, and green represent cement, water (pores), and tailings, respectively.

Moreover, the microstructure of the slurry has obvious fractal characteristics. Therefore, using fractal theory to analyze the structure quantitatively is feasible. On the basis of Moore's work [55], we adopt relative structure coefficient λ' to investigate the structural evolution of paste during mixing. λ' is related to the box-counting dimension, and it can be calculated through Eq. (4).

$$\lambda' = \frac{D_B(t) - D_{Bmin}}{D_{Bmax} - D_{Bmin}} \tag{4}$$

where $D_B(t)$ is the box dimension of the microstructure in the mixing, D_{Bmax} and D_{Bmin} are the maximum and minimum of $D_B(t)$, respectively.

When all the aggregate structures in the system are destroyed, the solid particles (tailings and cement) are uniformly distributed in the slurry, and then $D_{Bmin} = 1$. The range of λ' is 0–1. A large λ' indicates that particles connect with each other in the microstructure. Therefore, we set λ' at the initial time as 1, and $D_{Bmax} = D_B$ $(t = 0)$. Then, the λ' in Fig. 9(a–c) can be calculated as 0.97, 0.52, and 0.49, respectively.

5.2. Relationship between the rheological properties and microstructure of paste

To investigate the relationship between the rheological properties and microstructure of paste, the measurement of rheological properties is performed simultaneously for yield stress and viscosity determination at different times. The evolution of rheological properties and λ' with mixing time is shown in Fig. 10.

It illustrates that the yield stress and viscosity are consistent with the evolution trend of λ'. Both rheological properties and λ' decrease with mixing time first and then reach a stable state at approximately 5 min. Under the effect of shearing, the microstructure of paste is destroyed and λ' decreases, resulting in the reduction of yield stress and viscosity. Meanwhile, particles reconnect, and the microstructure is reconstructed. When the reconstruction rate is equal to the destroy rate, λ' becomes stable. Note that viscosity has an upward trend when the material is soaked at the beginning of mixing. After reaching the peak, it begins to decrease under the action of shear.

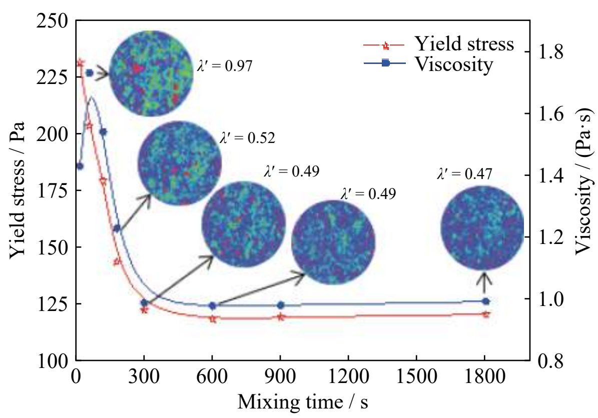

Fig. 10. Evolution of rheological properties and λ' with mixing time (modified from [12]).

The phenomenon that the rheological properties of paste decrease with mixing time is so-called shear thinning. However, in some special conditions, such as ultra-high shear, the shear thickening of the paste may occur [22].

6. Rheological behavior of paste in pipeline transportation

Paste flowing in the pipeline is regarded as "plug flow" due to high concentration [27]. Based on the Buckingham equation, the flow resistance of paste in the pipeline is always determined through Eq. (5) on the condition that the yield stress and plastic viscosity are known [9,24].

$$i = \frac{\Delta P}{L} = \frac{16}{3D}\tau_y + \frac{32v}{D^2}\eta_B \tag{5}$$

where i is the flow resistance, ΔP is the pressure drop, L is the pipeline length, D is the pipeline diameter, v is the velocity of paste, τ_y and η_B are the yield stress and viscosity of paste, respectively.

However, some key factors, including working conditions, environment, and transportation distance, affect the shear rate and the shear history of paste, resulting in changes in its rheological behavior, such as the shear thinning behavior of paste during long-distance transportation, the wall slip phenomenon caused by particle migration in a complex flow field, and the temperature effect of alpine regions on paste transportation [9,27,56–57]. Therefore, the flow resistance predicated by Eq. (5) is inconsistent with the actual situation, leading to pipeline accidents, such as vibration, pipeline-plugging, pipeline-wearing, and even pipeline explosion.

6.1. Influence of wall slip on pipeline transportation

Due to high yield stress and high plastic viscosity, the paste flows in laminar flow generally during the pipeline transportation process. According to apparent slip theory [58], the following assumptions are made for the paste laminar flow in the pipe: (1) the fluid in the slip layer has no slip on the pipeline wall; (2) the slip layer thickness is small and does not affect the viscosity characteristics of the main body of the slurry; (3) the slip layer thickness is the same everywhere on the wall and is unaffected by the pipeline size; (4) under laminar flow conditions, the shear stress from the center to the wall changes linearly along the radial direction.

The flow structure of paste under laminar flow conditions in a pipeline is shown in Fig. 11, where r_0 and R are the plug flow and pipeline, respectively. The radial shear stress τ of the paste is linearly distributed, with the maximum value at the wall and zero at the center. For the fluid with yield stress τ_y and the ponit with a distance r from the center of the pipe, it is assumed that when $r = r_0$, $\tau = \tau_y$, that is, $r_0 = \tau_y R / \tau_w$, where τ_w is the wall shear stress. Assuming that the thickness

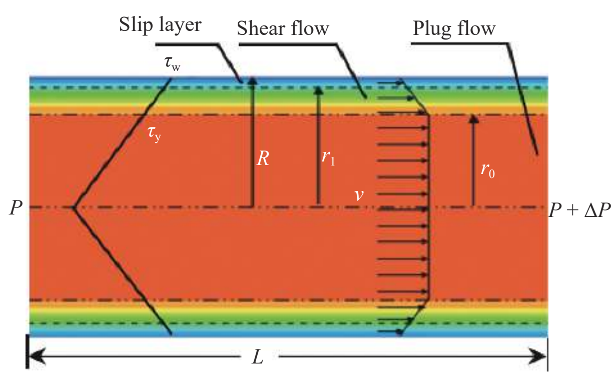

Fig. 11. Schematic of the wall slip in the pipeline transportation of paste (modified from [27]).

of the slip layer is δ, $r_1 = R - \delta$. In the range of $0 < r < r_0$, τ is less than τ_y. At this time, no shear deformation occurs, and the velocity of each point is the same. Thus, this part of the paste is in the plug flow zone. In the range of $r_0 < r < r_1$, τ is more than τ_y. This part of the paste is in the shear flow zone, and shear deformation occurs. A slip layer formed by particle migration occurs in the range of $r_1 < r < R$. This part of the paste is in the slip layer.

Therefore, the influence of wall slip on flow resistance should be considered. The flow resistance based on rheological properties and wall slip can be determined through Eq. (6) [12,56].

$$i = \frac{16}{3(8\beta_c\eta_B + D)}\tau_y + \frac{32v}{(8\beta_c\eta_B + D)D}\eta_B \tag{6}$$

where β_c is the slip coefficient, which is related to the thickness and viscosity of the slip layer.

6.2. Influence of time–temperature dependency on pipeline transportation

The rheological properties of paste are commonly known as time-dependent [22,59–62]. At the same time, the different temperatures generated from the geographic location of the mine, the friction between the pipeline and paste, the rock mass surrounding the pipeline, and the cement hydration may affect the rheological properties of paste [63–65]. Therefore, predicting the coupled effect of time and temperature on the rheological properties of paste and flow resistance is important [59–62].

The influence of time–temperature dependency on the yield stress and viscosity is described by Eqs. (7) and (8), respectively [9,12,61].

$$\tau_y(t,T) = \tau_{y0}(t_0,T_0)\exp\{-k[t + c_1(T-30)]\} \tag{7}$$

$$\eta_B(t,T) = \eta_{B0}(t_0,T_0) - m[t + c_2(T-30)] \tag{8}$$

where $\tau_y(t,T)$ and $\eta_B(t,T)$ are the yield stress and viscosity at thixotropic time t and temperature T; $\tau_{y0}(t_0,T_0)$ and $\eta_{B0}(t_0,T_0)$ are the yield stress and viscosity at the initial thixotropic time t_0 and reference temperature T_0; k and m are the thixotropic time parameter; c_1 and c_2 are the fitting coefficients.

Substituting Eqs. (7) and (8) into Eq. (5), the flow resistance considering time and temperature effect is obtained, as shown in Eq. (9) [9,12,61].

$$\begin{cases} i(t,T) = \dfrac{16}{3D}\tau_{y0}\exp\{-k[t + c_1(T-30)]\} + \\ \quad \dfrac{32v}{D^2}\{\eta_{B0} - m[t + c_2(T-30)]\}, \quad t \leqslant t_{total} \\ i(t,T) = i(t_{total},T), \quad t > t_{total} \end{cases} \tag{9}$$

where t_{total} is the thixotropic equilibrium time of paste. τ_{y0}, η_{B0}, k, m, c_1, c_2, and t_{total} are constants for a particular paste, which can be determined by rheological measurements.

Note that the number "30" in Eqs. (7) and (9) is a specific temperature value during the experiment [9,12,61], and it may be different for other pastes or experiments. Moreover, if we ignore the interaction between wall slip and time–temperature dependency, then we can substitute Eqs. (7) and (8) into Eq. (6) to investigate the coupling effect of wall slip and time–temperature dependency on pipeline transportation. The flow resistance can be determined by Eq. (10).

$$\begin{cases} i(t,T) = \dfrac{16}{3(8\beta_c\eta_B + D)}\tau_{y0}\exp\{-k[t + c_1(T-30)]\} + \\ \dfrac{32v}{(8\beta_c\eta_B + D)D}\{\eta_{B0} - m[t + c_2(T-30)]\}, \quad t \leqslant t_{\text{total}} \\ i(t,T) = i(t_{\text{total}}, T), \quad t > t_{\text{total}} \end{cases} \tag{10}$$

7. Rheological behavior of the filling body

After being transported to the underground goaf, paste slurry solidifies and hardens into the filling body, known as artificial low-strength rock. The filling body and surrounding rock form a unified geological body, as illustrated in Fig. 12.

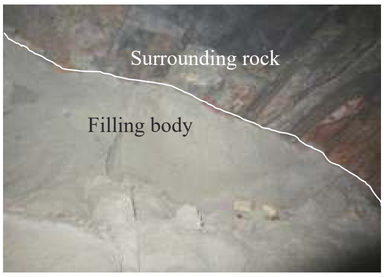

Fig. 12. Filling body in the underground goaf.

When the filling body is exposed to geological action, mining disturbance, or other external factors, it may be relatively stable after experiencing a period of deformation or may maintain a long continuous slow deformation (creep). However, the filling body may undergo a rapid deformation under the effect of blasting or another underground engineering and then experience another stable or creep period. Moreover, the filling body may be destroyed. At present, research on the rheological behavior of the filling body mainly focuses on the creep behavior, which consists of creep damage [66–68] and creep hardening [69]. Little attention is paid to stress relaxation, long-term strength, elastic after-effect, and flow of the filling body.

Compared with rock, the strength of the filling body is low because it has many pores. The creep damage of the filling body appears early under the action of stress. Therefore, considering the damage in the creep constitutive equation of the filling body is necessary. To define the damage with the change value of the deformation modulus, the damage variable $D(\sigma,t)$ is introduced on the basis of the effective stress model and the strain equivalence principle [68], as shown in Eq. (11).

$$D(\sigma,t) = 1 - \frac{1}{E(\sigma,t)}[E(\sigma,\infty) + (E(\sigma,0) - E(\sigma,\infty))e^{-\alpha t}] \tag{11}$$

where $D(\sigma,t)$ is the damage variable at loading time t, $E(\sigma,0)$ is the initial deformation modulus at the σ stress level, $E(\sigma, t)$ is the deformation modulus at the stress level σ and the loading time t, $E(\sigma,\infty)$ is the stable deformation modulus, e is Euler number, and α is the material parameter related to the stress level.

Substituting Eq. (11) into the Burgers model [70], we can obtain the improved constitutive equation of the Burgers model, as presented in Eq. (12) [68].

$$\varepsilon(t) = \frac{\sigma_0}{1 - D(\sigma,t)}\left[\frac{1}{E_M} + \frac{1}{\eta_M}t + \frac{1}{E_K}(1 - e^{-\frac{E_K}{\eta_K}t})\right] \tag{12}$$

where ε is the creep strain, σ_0 is the stress level, E_M and E_K are the deformation modulus, η_M and η_K are the viscosity coefficient.

The effects of loading time and stress level on the creep parameters are considered in Eq. (12), reflecting the phenomenon of parameters weakening with loading time and the law of damage and deterioration of the filling body. The creep damage can be explained by the macro–micro structure evolution of the filling body under the action of stress. Based on the CT scan images and simulation of the creep damage of the filling body, the creep damage can be divided into four stages: no microcrack region, initiation, and aggregation of microcrack; connection of microcrack; and formation of macroscopic fracture region [29,71].

8. Conclusions and future work

As a branch of rheology, paste rheology in metal mines has only been developed for over a decade. The study of paste rheology is extremely complicated due to its high concentration, the complexity of paste slurry materials, and the "three non" engineering characteristics. The rheological behavior of full tailings in deep thickening, paste in mixing and pipeline transportation, and the filling body are introduced and discussed in this paper.

However, in-depth and systematic studies are still needed to establish a complete theoretical system of paste rheology in metal mines. The following topics are proposed: standard for measuring the rheological properties of paste; constitutive equation of paste for the four key processes of CPB; combination of theoretical study, rheological experiments, numerical calculation, and AI (artificial Intelligence) modeling; application of paste rheology in the research and development of CPB technology and equipment.

Acknowledgements

This work was financially supported by the National Natural Science Foundation of China (Nos. 52130404 and 51774039), the Project funded by China Postdoctoral Science Foundation (No. 2021M690011), the Guangdong Basic and Applied Basic Research Foundation (No. 2021A 1515110161), and the Postdoctor Research Foundation of Shunde Graduate School of University of Science and Technology Beijing (No. 2021BH011). The authors want to thank all of the members of their research group, partners, and support units.

Conflict of Interest

The authors declare no conflicts of interest.

References

[1] C. Wang, D. Harbottle, Q.X. Liu, and Z.H. Xu, Current state of fine mineral tailings treatment: A critical review on theory and practice, *Miner. Eng.*, 58(2014), p. 113.

[2] J.C. Santamarina, L.A. Torres-Cruz, and R.C. Bachus, Why coal ash and tailings dam disasters occur, *Science*, 364(2019), No. 6440, p. 526.

[3] L.H. Silva Rotta, E. Alcântara, E. Park, R.G. Negri, Y.N. Lin, N. Bernardo, T.S.G. Mendes, and C.R. Souza Filho, The 2019 Brumadinho tailings dam collapse: Possible cause and impacts of the worst human and environmental disaster in Brazil, *Int. J. Appl. Earth Obs.*, 90(2020), art. No. 102119.

[4] J. Kiventerä, P. Perumal, J. Yliniemi, and M. Illikainen, Mine tailings as a raw material in alkali activation: A review, *Int. J. Miner. Metall. Mater.*, 27(2020), No. 8, p. 1009.

[5] C.C. Qi and A. Fourie, Cemented paste backfill for mineral tailings management: Review and future perspectives, *Miner. Eng.*, 144(2019), art. No. 106025.

[6] S.H. Yin, Y.J. Shao, A.X. Wu, H.J. Wang, X.H. Liu, and Y. Wang, A systematic review of paste technology in metal mines for cleaner production in China, *J. Clean. Prod.*, 247(2020), art. No. 119590.

[7] A.X. Wu, Y. Yang, H.Y. Cheng, S.M. Chen, and Y. Han, Status and prospects of paste technology in China, *Chin. J. Eng.*, 40(2018), No. 5, p. 517.

[8] Y.Y. Tan, E. Davide, Y.C. Zhou, W.D. Song, and X. Meng, Long-term mechanical behavior and characteristics of cemented tailings backfill through impact loading, *Int. J. Miner. Metall. Mater.*, 27(2020), No. 2, p. 140.

[9] H.Y. Cheng, S.C. Wu, H. Li, and X.Q. Zhang, Influence of time and temperature on rheology and flow performance of cemented paste backfill, *Constr. Build. Mater.*, 231(2020), art. No. 117117.

[10] A.X. Wu, Z.E. Ruan, R. Bürger, S.H. Yin, J.D. Wang, and Y. Wang, Optimization of flocculation and settling parameters of tailings slurry by response surface methodology, *Miner. Eng.*, 156(2020), art. No. 106488.

[11] A.X. Wu and H.J. Wang, *Theory and Technology of Cemented Paste Backfill in Metal Mines*, Science Press, Beijing, 2015.

[12] A.X. Wu, *Rheology of Paste in Metal Mines*, Metallurgical Industry Press, Beijing, 2019.

[13] General Administration of Quality Supervision, People's Republic of China, GB/T39489–2020: *Technical Specification for the Total Tailings Paste Backfill*, Standards Press of China, Beijing, 2020.

[14] F. Schoenbrunn and M. Bach, The development of paste thickening and its application to the minerals industry; An industry review, *BHM Berg Und Hüttenmännische Monatshefte*, 160(2015), No. 6, p. 257.

[15] H.Z. Jiao, A.X. Wu, H.J. Wang, S.P. Zhong, R.M. Ruan, and S.H. Yin, The solids concentration distribution in the deep cone thickener: A pilot scale test, *Korean J. Chem. Eng.*, 30(2013), No. 2, p. 262.

[16] J.C. Serbon, L. Mac-Namara, and F. Schoenbrunn, Application of the FLSmidth deep cone technology to the fertilizer plants in OCP, *Procedia Eng.*, 138(2016), p. 314.

[17] Z.E. Ruan, Y. Wang, A.X. Wu, S.H. Yin, and F. Jin, A theoretical model for the rake blockage mitigation in deep cone thickener: A case study of lead-zinc mine in China, *Math. Probl. Eng.*, 2019(2019), art. No. 2130617.

[18] Z.E. Ruan, A.X. Wu, R. Bürger, F. Betancourt, Y.M. Wang, Y. Wang, H.Z. Jiao, and S.K. Wang, Effect of interparticle interactions on the yield stress of thickened flocculated copper mineral tailings slurry, *Powder Technol.*, 392(2021), p. 278.

[19] Y. Wang, A.X. Wu, Z.E. Ruan, Z.H. Wang, Z.S. Wei, G.F. Yang, and Y.M. Wang, Reconstructed rheometer for direct monitoring of dewatering performance and torque in tailings thickening process, *Int. J. Miner. Metall. Mater.*, 27(2020), No. 11, p. 1430.

[20] H. Li, A.X. Wu, H.J. Wang, H. Chen, and L.H. Yang, Changes in underflow solid fraction and yield stress in paste thickeners by circulation, *Int. J. Miner. Metall. Mater.*, 28(2021), No. 3, p. 349.

[21] H.J. Wang, L.H. Yang, H. Li, X. Zhou, and X.T. Wang, Using coupled rheometer-FBRM to study rheological properties and microstructure of cemented paste backfill, *Adv. Mater. Sci. Eng.*, 2019(2019), art. No. 6813929.

[22] L.H. Yang, H.J. Wang, A.X. Wu, H. Li, A.B. Tchamba, and T.A. Bier, Shear thinning and thickening of cemented paste backfill, *Appl. Rheol.*, 29(2019), No. 1, p. 80.

[23] L.H. Yang, H.J. Wang, H. Li, and X. Zhou, Effect of high mixing intensity on rheological properties of cemented paste backfill, *Minerals*, 9(2019), No. 4, art. No. 240.

[24] T. Belem and M. Benzaazoua, Design and application of underground mine paste backfill technology, *Geotech. Geol. Eng.*, 26(2008), No. 2, p. 147.

[25] M. Fehrsen and R. Cooke, Paste fill pipeline distribution systems—Current status, [in] *Rise of the Machines—The 'State of the Art' in Mining Mechanisation, Automation, Hydraulic Transportation and Communications*, The South African Institute of Mining and Metallurgy, Johannesburg [2021-11-11]. https://www.saimm.co.za/Conferences/RiseOfMachines/026-Fehrsen.pdf

[26] J.W. Calderón-Hernández, A. Sinatora, H.G. de Melo, A.P. Chaves, E.S. Mano, L.S. Leal Filho, J.L. Paiva, A.S. Braga, and T.C. Souza Pinto, Hydraulic convey of iron ore slurry: Pipeline wear and ore particle degradation in function of pumping time, *Wear*, 450-451(2020), art. No. 203272.

[27] A.X. Wu, Z.E. Ruan, Y.M. Wang, S.H. Yin, S.Y. Wang, Y. Wang, and J.D. Wang, Simulation of long-distance pipeline transportation properties of whole-tailings paste with high sliming, *J. Cent. South Univ.*, 25(2018), No. 1, p. 141.

[28] Q.L. Zhang, Q.S. Chen, and X.M. Wang, Cemented backfilling technology of paste-like based on aeolian sand and tailings, *Minerals*, 6(2016), No. 4, art. No. 132.

[29] W. Sun, K.P. Hou, Z.Q. Yang, and Y.M. Wen, X-ray CT three-dimensional reconstruction and discrete element analysis of the cement paste backfill pore structure under uniaxial compression, *Constr. Build. Mater.*, 138(2017), p. 69.

[30] B.Q. Yan, F.H. Ren, M.F. Cai, and C. Qiao, Influence of new hydrophobic agent on the mechanical properties of modified cemented paste backfill, *J. Mater. Res. Technol.*, 8(2019), No. 6, p. 5716.

[31] A. Ghirian and M. Fall, Strength evolution and deformation behaviour of cemented paste backfill at early ages: Effect of curing stress, filling strategy and drainage, *Int. J. Min. Sci. Technol.*, 26(2016), No. 5, p. 809.

[32] E. Yilmaz and M. Fall, *Paste Tailings Management,* Springer, Cham, 2017.

[33] C.C. Qi, A. Fourie, Q.S. Chen, X.L. Tang, Q.L. Zhang, and R.G. Gao, Data-driven modelling of the flocculation process on mineral processing tailings treatment, *J. Clean. Prod.*, 196(2018), p. 505.

[34] C.C. Qi, Q.S. Chen, and S.S. Kim, Integrated and intelligent design framework for cemented paste backfill: A combination of robust machine learning modelling and multi-objective optimization, *Miner. Eng.*, 155(2020), art. No. 106422.

[35] S.H. Yin, A.X. Wu, K.J. Hu, Y. Wang, and Y.K. Zhang, The effect of solid components on the rheological and mechanical properties of cemented paste backfill, *Miner. Eng.*, 35(2012), p. 61.
[36] D. Feys, R. Cepuritis, S. Jacobsen, K. Lesage, E. Secrieru, and A. Yahia, Measuring rheological properties of cement pastes: Most common techniques, procedures and challenges, *RILEM Tech. Lett.*, 2(2017), p. 129.
[37] A.X. Wu, H. Li, H.Y. Cheng, Y.M. Wang, C.P. Li, and Z.E. Ruan, Status and prospects of researches on rheology of paste backfill using unclassified-tailings (Part 1): Concepts, characteristics and models, *Chin. J. Eng.*, 42(2020), No. 7, p. 803.
[38] B.H. Yan, C.P. Li, A.X. Wu, S.Y. Wang, and H.Z. Hou, Analysis on influencing factors of coarse particles migration in pipeline transportation of paste slurry, *Chin. J. Nonferrous Met.*, 28(2018), No. 10, p. 2143.
[39] B.H. Yan, C.P. Li, A.X. Wu, H.J. Wang, and H.Z. Hou, Analysis of law of movement of coarse aggregate particles in pipeline transportation of paste, *J. Cent. South Univ. Sci. Technol.*, 50(2019), No. 1, p. 172.
[40] L. Pullum, L. Graham, M. Rudman, and R. Hamilton, High concentration suspension pumping, *Miner. Eng.*, 19(2006), No. 5, p. 471.
[41] L. Pullum, D.V. Boger, and F. Sofra, Hydraulic mineral waste transport and storage, *Annu. Rev. Fluid Mech.*, 50(2018), p. 157.
[42] H.Y. Cheng, S.C. Wu, X.Q. Zhang, and A.X. Wu, Effect of particle gradation characteristics on yield stress of cemented paste backfill, *Int. J. Miner. Metall. Mater.*, 27(2020), No. 1, p. 10.
[43] A. Knight, F. Sofrà, A. Stickland, P. Scales, D. Lester, and R. Buscall, Variability of shear yield stress—Measurement and implications for mineral processing, [in] *Proceedings of the 20th International Seminar on Paste and Thickened Tailings*, Beijing, 2017.
[44] A.X. Wu, H. Li, H.Y. Cheng, Y.M. Wang, C.P. Li, and Z.E. Ruan, Status and prospects of research on the rheology of paste backfill using unclassified tailings (Part 2): Rheological measurement and prospects, *Chin. J. Eng.*, 43(2021), No. 4, p. 451.
[45] W. Mbasha, I. Masalova, R. Haldenwang, and A. Malkin, The yield stress of cement pastes as obtained by different rheological approaches, *Appl. Rheol.*, 25(2015), No. 5, art. No. 53517.
[46] H.J. Wang, Y. Wang, A.X. Wu, Y.G. Zhai, and H.Z. Jiao, Research of paste new definition from the viewpoint of saturation ratio and bleeding rate, *J. Wuhan Univ. Technol.*, 33(2011), No. 6, p. 85.
[47] S.P. Usher and P.J. Scales, Steady state thickener modelling from the compressive yield stress and hindered settling function, *Chem. Eng. J.*, 111(2005), No. 2-3, p. 253.
[48] R. Buscall and L.R. White, The consolidation of concentrated suspensions. Part 1.—The theory of sedimentation, *J. Chem. Soc., Faraday Trans. 1*, 83(1987), No. 3, p. 873.
[49] R.G. de Kretser, D.V. Boger, and P.J. Scales, Compressive rheology : An overview, *Rheol. Rev.*, 2003, p. 125.
[50] M. Rahimi, A.A. Abdollahzadeh, and B. Rezai, The effect of particle size, pH, and flocculant dosage on the gel point, effective solid stress, and thickener performance of a coal-washing plant, *Int. J. Coal Prep. Util.*, 35(2015), No. 3, p. 125.
[51] G.C. Li, *Study on Size Change of Unclassified Tailings Flocs and Its Thickening Performance* [Dissertation], University of Science and Technology Beijing, Beijing, 2019.
[52] G.J. Kynch, A theory of sedimentation, *Trans. Faraday Soc.*, 48(1952), p. 166.
[53] M. Nehdi and M.A. Rahman, Estimating rheological properties of cement pastes using various rheological models for different test geometry, gap and surface friction, *Cem. Concr. Res.*, 34(2004), No. 11, p. 1993.
[54] H.S. Coe and G.H. Clevenger, Methods for determining the capacities of slime-settling tanks, *Trans. Am. Inst. Min. Eng.*, 55(1916), p. 356.
[55] F. Moore, The rheology of ceramic slips and bodies, *Trans. J. Br. Ceram. Soc.*, (1959), 9. 470.
[56] A.X. Wu, X.H. Liu, H.J. Wang, H.Z. Jiao, and S.Z. Liu, Calculation of resistance in total tailings paste piping transportation based on time-varying behavior, *J. China Univ. Min. Technol.*, 42(2013), No. 5, p. 736.
[57] A.X. Wu, H.Y. Cheng, Y.M. Wang, H.J. Wang, X.H. Liu, and G.C. Li, Transport resistance characteristic of paste pipeline considering effect of wall slip, *Chin. J. Nonferrous Met.*, 26(2016), No. 1, p. 180.
[58] D.M. Kalyon, Apparent slip and viscoplasticity of concentrated suspensions, *J. Rheol.*, 49(2005), No. 3, p. 621.
[59] S. Haruna and M. Fall, Time- and temperature-dependent rheological properties of cemented paste backfill that contains superplasticizer, *Powder Technol.*, 360(2020), p. 731.
[60] W.B. Xu, Y.L. Zhang, X.H. Zuo, and M. Hong, Time-dependent rheological and mechanical properties of silica fume modified cemented tailings backfill in low temperature environment, *Cem. Concr. Compos.*, 114(2020), art. No. 103804.
[61] H.Y. Cheng, *Characteristics of Rheological Parameters and Pipe Resistance under the Time Temperature Effect* [Dissertation], University of Science and Technology Beijing, Beijing, 2018.
[62] D. Wu, M. Fall, and S.J. Cai, Coupling temperature, cement hydration and rheological behaviour of fresh cemented paste backfill, *Miner. Eng.*, 42(2013), p. 76.
[63] M. Fall, J.C. Célestin, M. Pokharel, and M. Touré, A contribution to understanding the effects of curing temperature on the mechanical properties of mine cemented tailings backfill, *Eng. Geol.*, 114(2010), No. 3-4, p. 397.
[64] Y. Wang, M. Fall, and A.X. Wu, Initial temperature-dependence of strength development and self-desiccation in cemented paste backfill that contains sodium silicate, *Cem. Concr. Compos.*, 67(2016), p. 101.
[65] Z. Aldhafeeri, M. Fall, M. Pokharel, and Z. Pouramini, Temperature dependence of the reactivity of cemented paste backfill, *Appl. Geochem.*, 72(2016), p. 10.
[66] H.Y. Ran, Y.X. Guo, G.R. Feng, T.Y. Qi, and X.J. Du, Creep properties and resistivity-ultrasonic-AE responses of cemented gangue backfill column under high-stress area, *Int. J. Min. Sci. Technol.*, 31(2021), No. 3, p. 401.
[67] Q.L. Chang, W.J. Tang, Y. Xu, and H.Q. Zhou, Research on the width of filling body in gob-side entry retaining with high-water materials, *Int. J. Min. Sci. Technol.*, 28(2018), No. 3, p. 519.
[68] Q. Zhou and J.H. Liu, Study on creep property and damage evolution of rich-water packing material for mining, *J. China Coal Soc.*, 43(2018), No. 7, p. 1878.
[69] S.J. Chen, X.Y. Liu, Y. Han, Y.H. Guo, and K.Q. Ren, Experimental study of creep hardening characteristic and mechanism of filling paste, *Chin. J. Rock Mech. Eng.*, 35(2016), No. 3, p. 570.
[70] N. Yildirim, S. Shaler, W. West, E. Gajic, and R. Edgar, The usability of Burger body model on determination of oriented strand boards' creep behavior, *Adv. Compos. Lett.*, 29(2020), art. No. 2633366X2093589.
[71] W. Sun, *Macro-micro Mechanical Behaviors of Subsidence Disposal Paste and Compatible Deformation Control* [Dissertation], University of Science and Technology Beijing, Beijing, 2016.